Heliyon 10 (2024) e35475

Contents lists available at ScienceDirect

Heliyon

journal homepage: www.cell.com/heliyon

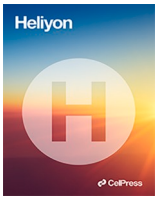

Research article

Quantitative proteomics and immunohistochemistry uncover NT5DC2 as a diagnostic biomarker for papillary urothelial carcinoma

Jun Yong Kim [a,1], Jae Seok Lee [b,1], Dohyun Han [c,d], Ilias P. Nikas [e], Hyeyoon Kim [c,d], Minsun Jung [a,**], Han Suk Ryu [f,g,*]

[a] Department of Pathology, Yonsei University College of Medicine, Seoul, 03722, Republic of Korea
[b] Department of Pathology, Samsung Changwon Hospital, Sungkyunkwan University School of Medicine, Changwon, 51353, Republic of Korea
[c] Transdisciplinary Department of Medicine and Advanced Technology, Seoul National University Hospital, Seoul, 03080, Republic of Korea
[d] Proteomics Core Facility, Biomedical Research Institute, Seoul National University Hospital, Seoul, 03080, Republic of Korea
[e] Medical School, University of Cyprus, Nicosia, 2029, Cyprus
[f] Seoul National University College of Medicine, Seoul, 03080, Republic of Korea
[g] Cancer Research Institute, Seoul National University, Seoul, 03080, Republic of Korea

ARTICLE INFO

Keywords:
Papillary urothelial carcinoma
Tandem mass spectrometry
Machine learning analysis
Biomarkers
Immunohistochemistry
Differential diagnosis

ABSTRACT

The accurate diagnosis of papillary urothelial carcinoma (PUC) is frequently challenging due to benign mimickers. Other than morphology-based diagnostic criteria, reliable biomarkers for differentiating benign and malignant papillary urothelial neoplasms remain elusive, so we sought to discover new markers to address this challenge. We first performed tandem mass spectrometry-based quantitative proteomics using diverse papillary urothelial lesions, including PUC, urothelial papilloma (UP), inverted urothelial papilloma, and cystitis cystica. We prioritized potential diagnostic biomarkers using machine learning, and subsequently validated through immunohistochemistry (IHC) in two independent cohorts. Metabolism, transport, cell cycle, development, and immune response functions were differentially enriched between malignant and benign papillary neoplasms. RhoB and NT5DC2 were shortlisted as optimal candidate markers for PUC diagnosis. In our pilot study using IHC, NT5DC2 was subsequently selected as its expression consistently differed in PUC ($p = 0.007$). Further validation of NT5DC2 using 49 low-grade (LG) urothelial lesions, including 15 LG-PUCs and 17 UPs, which are the most common mimickers, concordantly revealed lower IHC expression levels in LG-PUC ($p = 0.0298$). Independent external validation with eight LG-PUCs and eight UPs confirmed the significant downregulation of NT5DC2 in LG-PUC ($p = 0.0104$). We suggest that NT5DC2 is a potential IHC biomarker for differentiating LG-PUC from its benign mimickers, especially UP.

* Corresponding author. Department of Pathology, Seoul National University College of Medicine, 103 Daehak-ro, Jongno-gu, Seoul, 03080, Republic of Korea.
** Corresponding author. Department of Pathology, Yonsei University College of Medicine, Yonsei-ro 50-1, Seodaemun-gu, Seoul, 03722, Republic of Korea.
E-mail addresses: jjunglammy@yuhs.ac (M. Jung), nash77@snu.ac.kr (H.S. Ryu).
[1] Jun Yong Kim and Jae Seok Lee equally contributed to this work as the first authors.

https://doi.org/10.1016/j.heliyon.2024.e35475
Received 23 April 2024; Received in revised form 27 June 2024; Accepted 29 July 2024
Available online 30 July 2024

1. Introduction

Urothelial carcinoma (UC) is the most common malignancy of the urinary bladder and the 9th most common cancer worldwide [1]. Histopathologic examination remains the gold standard for the diagnosis of papillary urothelial carcinoma (PUC). However, differentiating low-grade PUC (LG-PUC) from benign urothelial neoplasms is often challenging because LG-PUC shows only mild nuclear atypia and low architectural disorder [2], while a spectrum of benign papillary urothelial lesions, including urothelial papilloma (UP), inverted urothelial papilloma (IUP), and cystitis cystica (CC), can mimic LG-PUC. The use of common immunohistochemical (IHC) markers, such as Ki-67, p53, cytokeratin 20 and HER2, has been proposed to facilitate high-grade PUC diagnosis in a context-dependent manner [3]. Recently, we revealed a novel protein marker distinguishing PUC with inverted growth from IUP [4]. However, it is still unknown how various benign and malignant papillary urothelial neoplasms can be differentiated within research or routine diagnostics.

Recent advances in quantitative proteomics have enabled researchers to analyze the biological characteristics of cancers and translate them into the clinic [5,6], revealing a direct association with cellular functions, unlike genomic or transcriptomic analyses. Furthermore, the proteomic approach has the advantage of discovering novel and promising biomarkers, which can be further validated with IHC and subsequent application in diagnostic pathology. In previous studies, we discovered novel diagnostic markers of UC using proteomic analysis of urine cytology and fresh-frozen paraffin-embedded (FFPE) specimens [4,7–9]. In this study, we performed proteomic analysis of selected papillary urothelial neoplasms to discover distinguishing biofunctions of PUC, in addition to a promising IHC biomarker for the histopathological diagnosis of LG-PUC.

2. Materials and methods

2.1. Sample selection

For proteomic analysis, papillary urothelial neoplasms and non-neoplastic urothelial tissues obtained by transurethral resection of the bladder (TURB) were selected from the Pathology Department of the Seoul National University Hospital (SNUH) (n = 10). They were divided into a PUC group (n = 5) and a benign group (n = 5); the latter included UP, IUP, and CC tissues. Among the PUC group, there were two cases with lamina propria invasion. Six out of these 10 specimens had not been previously analyzed in any of our previous studies (Supplementary Table S1). None of the patients had a previous history of UC or intravesical treatment.

We validated our findings on PUC and papillary urothelial lesions using IHC in two independent cohorts. The first cohort included 49 TURB specimens from the Pathology Department of the Severance Hospital, nine of which were also included in a pilot study. Furthermore, we analyzed 16 TURB tissues from SNUH to validate our selected IHC biomarker for distinguishing LG-PUC from UP. Every diagnosis was reviewed and graded according to the World Health Organization Classification [10]. All LG-PUCs were in grade 1. Clinical information was extracted from the patients' electronic medical records. The regional Institutional Review Boards (IRBs) of both hospitals approved the experimental protocols (IRB No. H-2009-163-1160 and 4-2022-0685). See Supplementary Table S2 and Supplementary Table S3 for details on the validation cohorts.

2.2. Liquid chromatography with tandem mass spectrometry and data analysis

Liquid chromatography with tandem mass spectrometry (LC-MS/MS) analysis was performed as previously described [4,7,9,11]. Target areas composed mainly of urothelium were selected and macro-dissected from unstained FFPE slides. Samples underwent filter-aided preparation and desalting before the LC-MS/MS-based proteomic analysis using a Q Exactive HF-X Hybrid Quadrupole-Orbitrap mass spectrometer (Thermo Fisher Scientific, Waltham, MA, USA) and an Ultimate 3000 RSLC system (Dionex, Sunnyvale, CA, USA), following the manufacturer's instructions. The MaxQuant.Live version 1.2 (Max Planck Institute of Biochemistry, Munich, Germany) was used to perform BoxCar acquisition [12]. The MS1 resolution was set to 120,000 at m/z 200 for BoxCar, and the acquisition cycle comprised two BoxCar scans at 12 boxes (scaled width, 1 Th overlap) with a maximum ion injection time of 20.8 per box and the individual Automatic Gain Control target set to 250,000. The MaxQuant version 1.6.1.0 was employed with the Andromeda engine to process the MS raw files [13,14]. The BoxCar was set as the experimental type in the global parameter. Otherwise, all search parameters were set as the default parameter of the software. The iBAQ algorithm was used as part of the MaxQuant platform for label-free quantification [15]. Raw LC–MS/MS data were uploaded into the PRIDE database (Accession ID: PXD027602), including benign samples, being reported for the first time.

2.3. Bioinformatic analysis of the proteomic data

Proteomic data analysis utilized Perseus software (Max Planck Institute of Biochemistry). Gene Ontology Biologic Process (GOBP) and Gene Ontology Molecular Functions (GOMFs) annotations were explicated using the Toppgene Suite [16]. GOBP annotations were also demonstrated using the single sample gene set enrichment analysis (ssGSEA) module (v10.0.1) [17].

2.4. Validation of candidate diagnostic biomarkers of PUC

We first screened candidate biomarkers using The Human Protein Atlas (https://www.proteinatlas.org/) [18]. Concisely, in each protein section of The Human Protein Atlas, the tissue tab provides IHC results for normal tissues, whereas the pathology tab for cancer

tissues. In these tabs, the IHC result of each protein in normal and cancer tissues is available as intensity scores (high, score 4; medium, score 3; low, score 2; not detected, score 1). For this particular analysis, we compared the intensity scores of normal urothelial cells and UCs. Biomarkers showing no significant difference (two-sided *t*-test p-value >0.05) between UC and benign urothelium were excluded. Supplementary Table S4 contains details of the antibodies used in the Human Protein Atlas [18].

Subsequently, we performed IHC assays for the shortlisted NT5DC2 (orb312336, Biorbyt Ltd, Cambridge, UK) and RhoB (sc-8048, Santa Cruz Biotechnology, Dallas, TX, USA) candidate biomarkers using the Ventana Benchmark platform (Ventana Medical Systems, Tucson, AZ, USA). IHC expression of NT5DC2 and RhoB was measured by the histo-score (H-score) [1 * (% cells 1+) + 2 * (% cells 2+) + 3 * (% cells 3+)], using the QuPath version 0.2.3 [19]. All IHC assays were analyzed in the urothelial epithelium, excluding stromal cells or inflammatory cells.

2.5. Statistics

Proteome abundance was compared using a two-sided *t*-test or Analysis of variance with a permutation-based false discovery rate (FDR) at significance level <0.05. We selected the top 100 upregulated and downregulated groups from the GOBP list using ssGSEA with an FDR <0.05, followed by hierarchical clustering using Euclidean distance as the metric. H-scores of each biomarker were compared using the Mann-Whitney test in Prism version 9.4.1 (GraphPad Software, LLC, San Diego, CA, USA). The area under the receiver operating characteristic (ROC) curve (AUC) was calculated using R (version 4.2.1), specifically the pROC package. The optimal H-score level with its corresponding sensitivity and specificity were determined using the Youden index.

3. Results

3.1. Proteomic signature is different in PUC compared to benign urothelial lesions

We selected 10 TURB samples for proteomic analysis (Supplementary Table S1), and Fig. 1A shows representative images. Using LC-MS/MS, we identified 9890 proteins, with 4945 quantified in five or more samples at a high confidence level (FDR <0.01). The normalized protein quantities are presented in the Supplementary Table S5. We identified 392 differentially expressed proteins (DEPs) between the PUC and benign groups using a two-sided *t*-test ($p < 0.05$, $|\text{fold change}| > 1.5$); 208 were upregulated, whereas 182 were downregulated in the PUC group, respectively (Fig. 1B and Supplementary Table S6). HLA-C protein, found in both upregulated and downregulated groups, was excluded for further analysis. Hierarchical clustering showed coherent separation between PUC and benign groups based on protein expression (Fig. 1C). We also investigated the biological processes associated with proteomes. GOBP analysis revealed enrichment of metabolism, cellular component organization, localization/intracellular transport and cell cycle (Fig. 1D). We performed ssGSEA using the GOBP and hallmark gene sets of the Molecular Signature Database files, revealing upregulated and downregulated GOBPs in the PUC group (Supplementary Table S7). The GOBP categories of viral process, metabolism, transport, immune, cell death and response to stimulus were significantly upregulated in the PUC group (FDR <0.05) (Fig. 1E), while response to stimulus, development, and organization were significantly downregulated (FDR <0.05) (Fig. 1F).

3.2. Candidate biomarkers for the diagnosis of PUC, identified by machine learning analysis

Based on the LC-MS/MS protein abundance, we conducted machine learning analysis to identify potential protein biomarkers dividing PUC and benign groups. To find differential proteomes between these two groups, we performed a feature selection method for support vector machine with a radial basis function kernel. Keeping the protein list short, the lowest error rates were achieved at 10 % between the PUC and benign groups with corresponding proteins. Consequently, we identified seven proteins including solute carrier family 25 member 36 (SLC25A36), Rho-related GTP-binding protein RhoB (RhoB), mitochondrial import inner membrane translocase subunit Tim17 B (Tim17 B), 5′-nucleotidase domain-containing protein 2 (NT5DC2), transcription factor 20 (TCF20), eosinophil cationic protein (ECP) and Charcot-Leyden crystal protein (CLC) (Fig. 2A). We also found GOBPs and GOMFs were implicated in the proteome set as follows: mitochondrial transmembrane transport, pyrimidine nucleotide transport and pyrimidine nucleotide import in GOBPs, while transmembrane transporter activity and enzymes activity including ribonuclease, hydrolase, nucleotidase, endopeptidase, endonuclease and lysophospholipase in GOMFs (Fig. 2B).

3.3. Candidate biomarkers for the diagnosis of LG-PUC, as identified by The Human Protein Atlas and a pilot study

From the seven candidates prioritized based on the machine learning rank order (Fig. 3A), we selected five proteins that were also included in the DEP list (Fig. 3B). Then, using public datasets of The Human Protein Atlas for the five candidate proteins, we compared the estimated IHC staining intensity of several UCs and normal urothelial tissues. We found that NT5DC2 expression showed a significant difference between UCs and normal urothelial tissues (Mann-Whitney $p = 0.014$), in contrast to Tim17 B, SLC25A36, and TCF20 (Fig. 3C). No data were available for RhoB expression in the database. Subsequently, NT5DC2 and RhoB were ultimately subjected to validation using IHC. On a pilot study enrolling 14 urothelial lesions, including PUC and benign lesions (UP, IUP and CC), the H-scores of NT5DC2 were significantly lower in PUC ($p = 0.007$), while RhoB showed no significant difference ($p = 0.8175$) (Fig. 3D). Specifically, both high-grade PUC (HG-PUC) ($p = 0.0317$) and LG-PUC ($p = 0.0317$) exhibited lower levels of NT5DC2 than the benign group (Fig. 3E). Thus, NT5DC2 was chosen as the final candidate biomarker distinguishing PUC from benign papillary urothelial lesions.

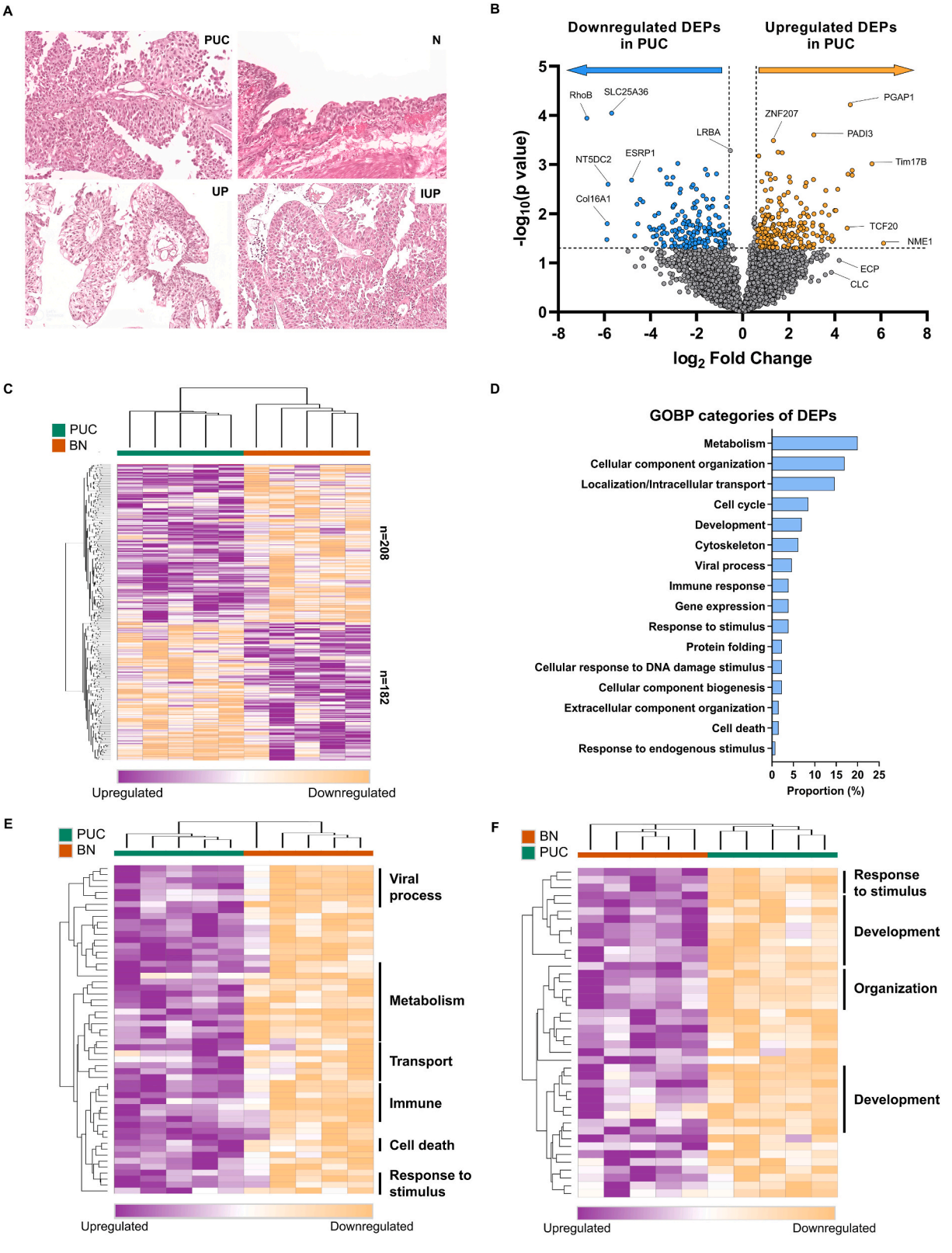

(caption on next page)

Fig. 1. Proteomics-based oncologic signatures of papillary urothelial carcinomas (PUCs) and benign urothelial lesions (BNs). (A) Representative images of selected PUC and BNs used for our proteomics analysis (200x). (B) Differentially expressed proteins (DEPs) that were significantly upregulated (n = 209) or downregulated (n = 182) in the PUC group using a *t*-test. (C) The PUC and benign groups clustered closely within the DEPs. (D) Gene Ontology-biologic process (GOBP) categories associated to the DEPs. (E–F) Unsupervised hierarchical clustering of differentially expressed GOBP signatures that were upregulated (E) or downregulated (F) in the PUC group. (Abbreviations: UP, urothelial papilloma; IUP, inverted urothelial papilloma; N, normal urothelial tissue).

3.4. NT5DC2 distinguishes LG-PUC from benign urothelial lesions, including UP

Given the greater challenge in differentiating benign or low-grade malignant lesions compared to HG-PUC, we further investigated the ability of NT5DC2 to differentiate LG-PUC from UP, IUP and CC in two independent cohorts. In the cohort of the Severance Hospital, comparing LG-PUC with the entire benign group revealed significantly lower NT5DC2 H-scores for LG-PUC ($p = 0.0298$) (Fig. 4A). When comparing individually, LG-PUC had significantly lower NT5DC2 expression than UP ($p = 0.0331$) and CC ($p = 0.0005$) (Fig. 4B), whereas LG-PUC and IUP showed no significant difference ($p = 0.1317$). IHC expression of NT5DC2 showed good performance in the diagnosis of LG-PUC over all benign group (AUC = 0.694 $p = 0.0298$) (Supplementary Fig. S1). Concerning differentiation between UP and LG-PUC represents common diagnostic difficulty in routine pathology practice [20], we further evaluated the ability of NT5DC2 for this purpose, which demonstrated good performance (AUC = 0.722, $p = 0.0331$) (Fig. 4C). We additionally enrolled 16 specimens (8 LG-PUCs and 8 UPs; SNUH cohort) and expression of NT5DC2 were found significantly lower in LG-PUCs than UPs ($p = 0.0104$) (Fig. 4D). By combining Severance and SNUH cohorts, the optimal cut-off of the NT5DC2 H-score at 128.17 achieved high sensitivity (=0.826) and specificity (=0.680) for the diagnosis of LG-PUC over UP (AUC = 0.739, $p = 0.004$) (Fig. 4E).

4. Discussion

In this study, we used quantitative proteomics and revealed proteomic landscapes of a spectrum of papillary urothelial lesions. Our research offers the benefit of uncovering the novel IHC biomarker NT5DC2, which aids in distinguishing LG-PUC from benign mimickers, especially UP.

We revealed distinct proteomic profiles of PUC, characterized by enrichment in metabolism, transport, cell cycle, and development. Specifically, PUC showed upregulated functions related to viral process, metabolism, transport, immune and cell death, while it showed downregulation in categories related to development and organization. The category response to stimulus was observed in both sides, but the side upregulated in PUC demonstrated stronger association with responses to exogenous organisms, like bacteria or viruses. The observed upregulation of immune, metabolism and cell death biologic processes aligns with previous studies [21]. Transport has also been reported previously as a process that can be upregulated in UCs [22]. Enrichment in viral-associated GOBPs may be attributed to the mutation pattern in UC, characterized by high rate-somatic mutations dominated by APOBEC mutagenesis, and the cytidine deaminase, an enzyme responsible for the innate immunity against retroviruses and retrotransposons, is known to be active in this process [23]. The upregulated GOBPs in the benign group, development, and organization consistently reflects the differentiated nature of the non-neoplastic tissue.

For the first time, we introduce NT5DC2 as a novel IHC biomarker to help differentiating LG/grade 1-PUC from UP, one of the commonest diagnostic challenges of urologic pathology [20]. While studies have investigated markers such as p53, Ki-67, CK20, and E-cadherin for diagnosing LG-PUC, their utility in the diagnostic process has been limited [24]. Diagnosing LG-PUC cannot still rely solely on the NT5DC2 expression; nevertheless, it offers valuable assistance when morphology alone fails to provide clear differentiation. We presented an optimal H-score of 128.17, which roughly corresponded to weak-to-moderate staining in most tumor cells or strong immunoreaction in 40% of tumor cells. This is especially noteworthy given the lack of practical markers for distinguishing between these two entities.

NT5DC2 functions as a hydrolase digesting nucleic acids, yet its implication in tumorigenesis remains poorly understood. NT5DC2 expression and its role have been investigated in various other types of cancer, including hepatocellular carcinoma [25], non-small cell lung cancer [26], and colorectal carcinoma [27]. In these studies, upregulation of NT5DC2 was related to cancer progression and poor prognosis, contrary to our finding in PUC. Further research is required to comprehend the pathological roles of NT5DC2 in PUC.

Other than NT5DC2, we identified additional candidate biomarkers using machine learning and DEP analysis, including RhoB, Tim17 B, SLC25A36, and TCF20. RhoB, a Rho GTP-binding family protein, is involved in various cellular functions [28,29]. While a tumor associated role of RhoB was reported in UC, additional research is needed to clarify its mechanism of action, especially given varying results in different cancer types [30–32]. Tim17 B and SLC25A36 are commonly involved in mitochondrial transport [33,34], and TCF20 is linked to neurodevelopmental or neurologic disorders through mutation [35]. However, their relationship with cancer also remains unclear.

There are some limitations of this study. We used 10 samples for proteomic analysis, which is a relatively small given the variety of tumors studied. Future research may benefit from including papillary urothelial neoplasm of low malignant potential to address diagnostic challenges more effectively.

In conclusion, we showed a distinctive proteome signature of PUC in comparison with benign urothelial lesions and identified NT5DC2 as a novel IHC biomarker with the potential to distinguish LG-PUC and UP. We anticipate that this IHC biomarker may aid pathologists in making accurate diagnoses in challenging cases.

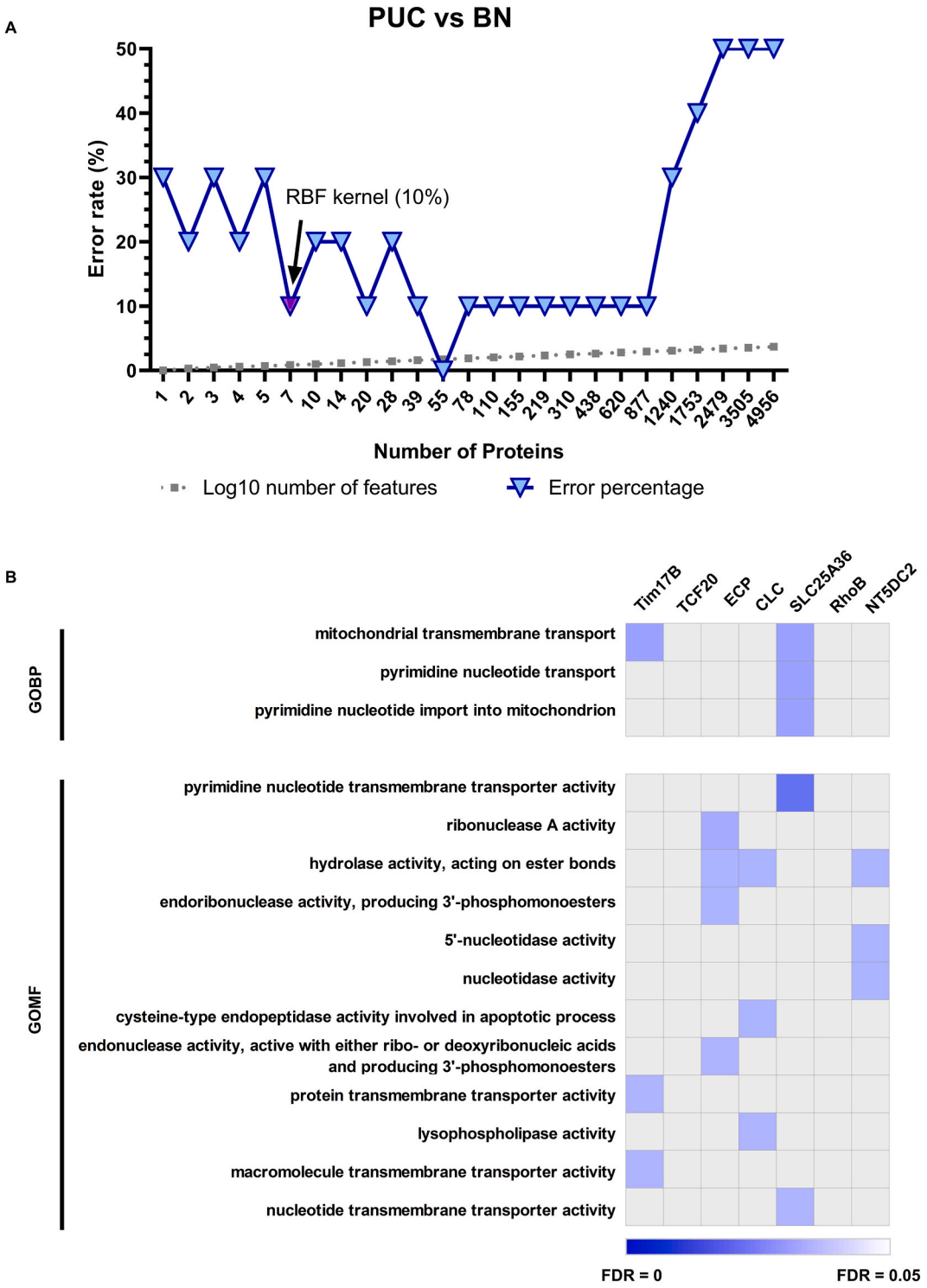

Fig. 2. Biomarker discovery for the diagnosis of papillary urothelial carcinoma (PUC). (A) Support vector machine identified seven biomarkers differentiating PUC from benign urothelial lesions (BNs). (B) Gene Ontology-biologic processes (GOBPs) and Gene Ontology-molecular functions (GOMFs) enriched in the seven candidate biomarkers for PUC diagnosis. Gray color indicates unrelated genes.

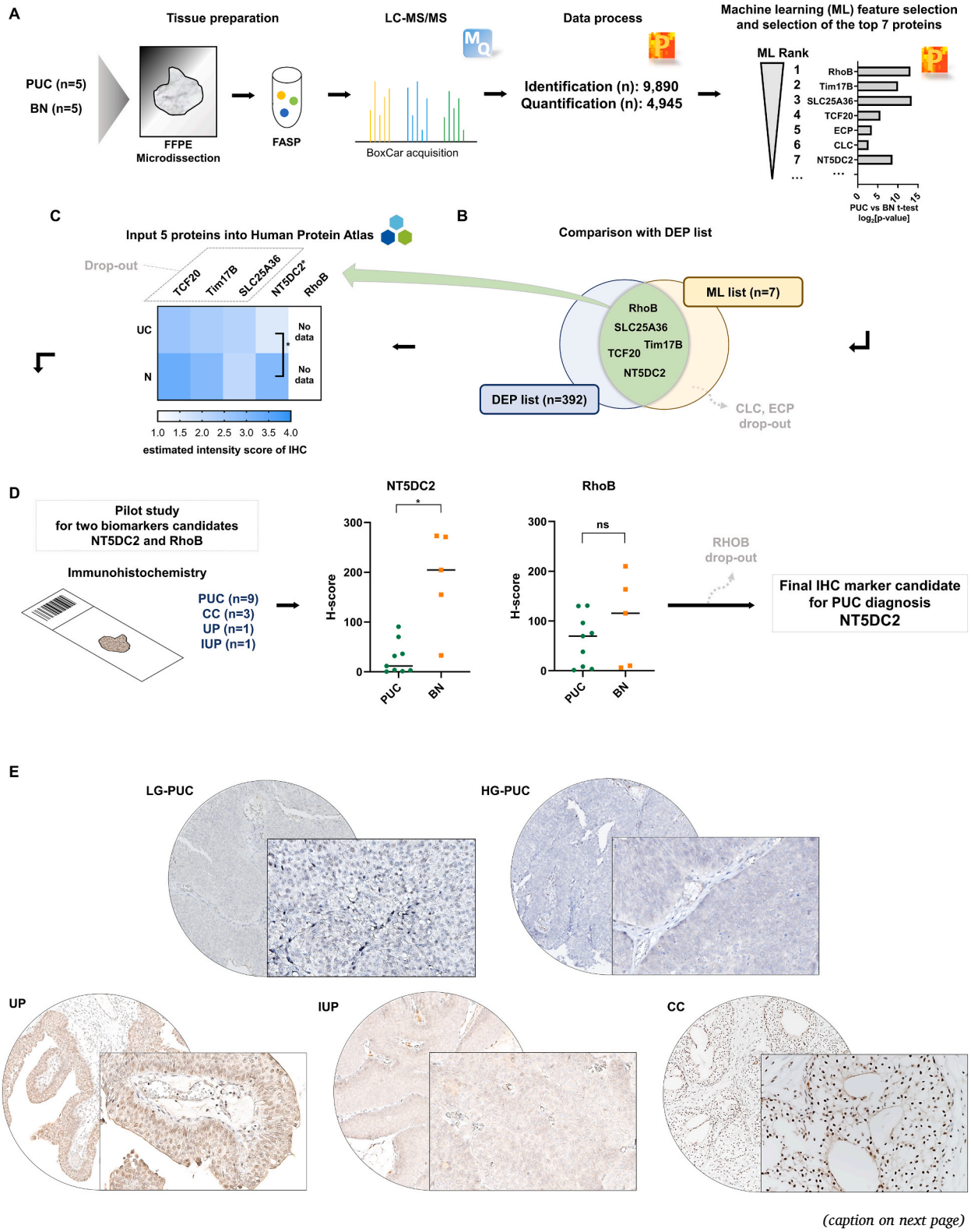

(caption on next page)

Fig. 3. Identification of NT5DC2 as a candidate biomarker for low-grade papillary urothelial carcinoma (LG-PUC) diagnosis. (A) Quantitative proteomics and machine learning-based feature selection of the seven candidate biomarkers to differentiate PUC from benign urothelial lesions. (B) Selection of five top-ranked proteins through cross-comparison with the differentially expressed proteins. (C) Narrowing down of the five proteins using published data of The Human Protein Atlas. TCF20, Tim17 B, and SLC25A36, which were similarly expressed in urothelial carcinoma (UC) and normal urothelium (N) in the Human Protein Atlas, were abandoned. NT5DC2 immunohistochemical expression differed between UC and N (*p = 0.014). Data for the expression of RhoB was not available. (D) In our pilot study using IHC, the H-scores of NT5DC2 and RHOB measured by digital pathology were compared with the Mann-Whitney test, confirming NT5DC2 as the final candidate biomarker (NT5DC2, p = 0.0317; RhoB, p = 0.8175). (E) Representative images of NT5DC2 immunostaining. Note that only nuclear staining was measured for this study, as nuclear staining was more conspicuous than cytoplasmic staining in our specimens (circles, 100x and squares, 400x). (Abbreviations: BN, benign urothelial lesion; CC, cystitis cystica; IUP, inverted papilloma; UP, urothelial papilloma).

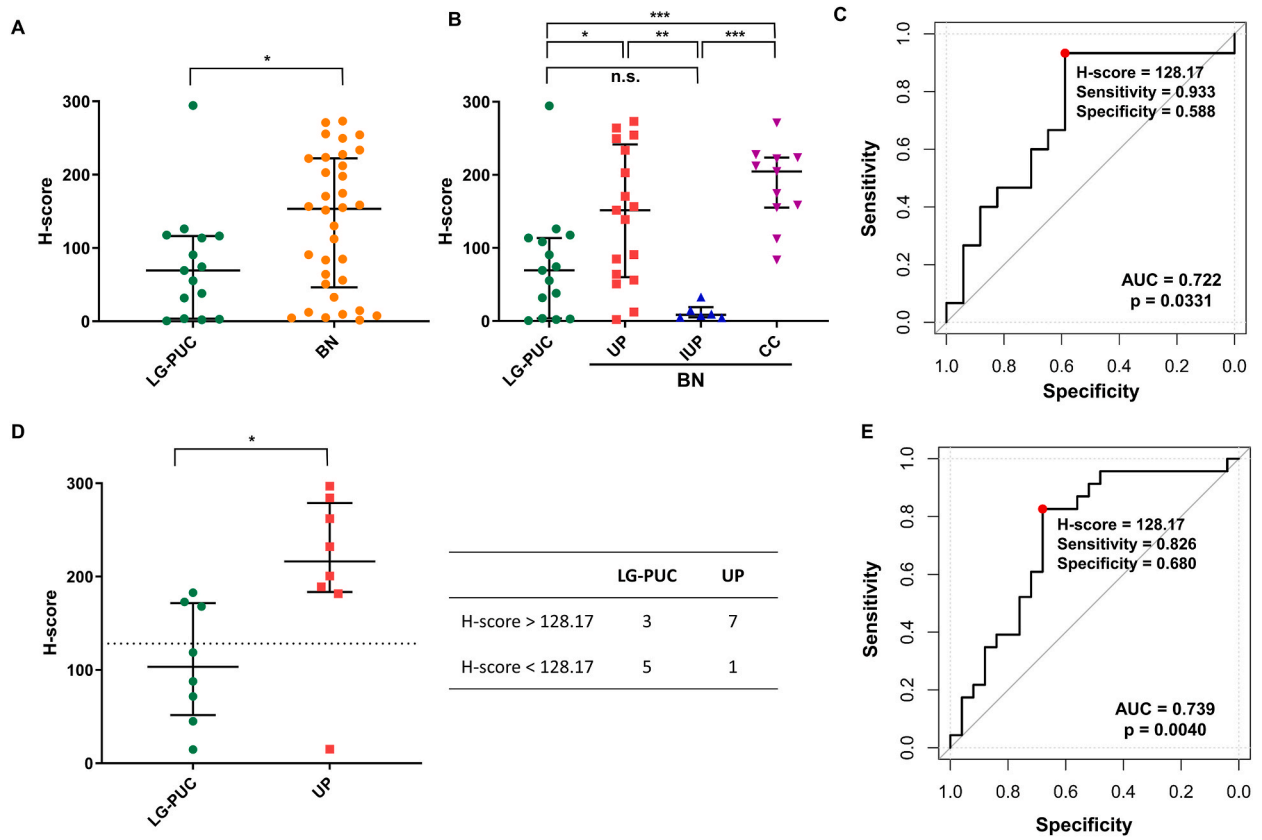

Fig. 4. Final validation of NT5DC2 immunostaining for low-grade papillary urothelial carcinoma (LG-PUC) diagnosis in two independent cohorts (Severance Hospital and SNUH). (A) NT5DC2 H-scores of LG-PUCs were significantly lower than the other benign urothelial lesions (BNs) in the Severance Hospital cohort (*p = 0.0298). (B) Comparison of the NT5DC2 H-scores among each entity in the Severance Hospital cohort. H-scores of LG-PUC were significantly lower than those of urothelial papilloma (UP) (*p = 0.0331) and cystitis cystica (CC) (***p = 0.0004), while the H-scores of inverted urothelial papilloma (IUP) were not significantly different from PUC. (C) ROC curve of NT5DC2 immunostaining to diagnose LG-PUC over UP showed high sensitivity (sensitivity = 0.933). (D) Comparison of the NT5DC2 H-scores between PUC and UP in the SNUH cohort showed a significant difference (*p = 0.0104). Applying the threshold calculated through the ROC curve (H-score = 128.17) to the external validation group to divide PUC and UP (sensitivity = 0.625 and specificity = 0.875). Note that positive test indicates a low H-score in this image (Mann-Whitney test *p < 0.05, **p < 0.01, ***p < 0.001).

Data availability statement

Data available at PRIDE database (Accession ID: PXD027602).

No conflicts of interest were declared.

All experimental protocols involving human subjects were approved by the Institutional Review Board (IRB No. H-2009-163-1160 at Seoul National University Hospital and 4-2022-0685 at Severance Hospital).

CRediT authorship contribution statement

Jun Yong Kim: Writing – original draft, Visualization, Validation, Formal analysis. **Jae Seok Lee:** Validation, Resources, Investigation, Funding acquisition, Data curation. **Dohyun Han:** Software, Resources, Formal analysis, Data curation. **Ilias P. Nikas:** Software, Resources, Funding acquisition. **Hyeyoon Kim:** Software, Resources, Formal analysis, Data curation. **Minsun Jung:** Writing – review & editing, Supervision, Methodology, Funding acquisition, Conceptualization. **Han Suk Ryu:** Supervision, Project administration, Methodology, Funding acquisition, Conceptualization.

Declaration of competing interest

The authors declare that they have no known competing financial interests or personal relationships that could have appeared to influence the work reported in this paper.

Acknowledgements

This research was funded by the National Research Foundation of Korea (NRF) funded by the Ministry of Science, ICT and Future Planning (2022R1C1C1006813). This work was also supported by the NRF grant funded by the Korea government (MSIT) (RS-2024-00341570).

Appendix A. Supplementary data

Supplementary data to this article can be found online at https://doi.org/10.1016/j.heliyon.2024.e35475.

References

[1] S. Antoni, J. Ferlay, I. Soerjomataram, A. Znaor, A. Jemal, F. Bray, Bladder cancer incidence and mortality: a global overview and recent trends, Eur. Urol. 71 (2017) 96–108.
[2] J.I. Epstein, M.B. Amin, V.R. Reuter, F.K. Mostofi, The World Health organization/international society of urological pathology consensus classification of urothelial (transitional cell) neoplasms of the urinary bladder. Bladder consensus conference committee, Am. J. Surg. Pathol. 22 (1998) 1435–1448.
[3] M.B. Amin, S.C. Smith, V.E. Reuter, J.I. Epstein, D.J. Grignon, D.E. Hansel, et al., Update for the practicing pathologist: the International Consultation on Urologic Disease-European association of urology consultation on bladder cancer, Mod. Pathol. 28 (2015) 612–630.
[4] M. Jung, C. Lee, D. Han, K. Kim, S. Yang, I.P. Nikas, et al., Proteomic-based machine learning analysis reveals PYGB as a novel immunohistochemical biomarker to distinguish inverted urothelial papilloma from low-grade papillary urothelial carcinoma with inverted growth, Front. Oncol. 12 (2022) 841398.
[5] M. Harel, R. Ortenberg, S.K. Varanasi, K.C. Mangalhara, M. Mardamshina, E. Markovits, et al., Proteomics of melanoma response to immunotherapy reveals mitochondrial dependence, Cell 179 (2019) 236–250 e218.
[6] L. Beck, M. Harel, S. Yu, E. Markovits, B. Boursi, G. Markel, et al., Clinical proteomics of metastatic melanoma reveals profiles of organ specificity and treatment resistance, Clin. Cancer Res. 27 (2021) 2074–2086.
[7] J.H. Park, C. Lee, D. Han, J.S. Lee, K.M. Lee, M.J. Song, et al., Moesin (MSN) as a novel proteome-based diagnostic marker for early detection of invasive bladder urothelial carcinoma in liquid-based cytology, Cancers (Basel) 12 (2020) 1018.
[8] H. Lee, K. Kim, J. Woo, J. Park, H. Kim, K.E. Lee, et al., Quantitative proteomic analysis identifies AHNAK (neuroblast differentiation-associated protein AHNAK) as a novel candidate biomarker for bladder urothelial carcinoma diagnosis by liquid-based cytology, Mol. Cell. Proteomics 17 (2018) 1788–1802.
[9] B. Kim, M. Jung, K.C. Moon, D. Han, K. Kim, H. Kim, et al., Quantitative proteomics identifies TUBB6 as a biomarker of muscle-invasion and poor prognosis in bladder cancer, Int. J. Cancer 152 (2023) 320–330.
[10] E.M. Comperat, M. Burger, P. Gontero, A.H. Mostafid, J. Palou, M. Roupret, et al., Grading of urothelial carcinoma and the new "World Health organisation classification of tumours of the urinary system and male genital organs 2016", Eur. Urol. Focus 5 (2019) 457–466.
[11] J.Y. Kim, D. Han, H. Kim, M. Jung, H.S. Ryu, The proteomic landscape shows oncologic relevance in cystitis glandularis, J. Pathol. Transl. Med. 57 (2023) 67–74.
[12] C. Wichmann, F. Meier, S. Virreira Winter, A.D. Brunner, J. Cox, M. Mann, MaxQuant.Live enables global targeting of more than 25,000 peptides, Mol. Cell. Proteomics 18 (2019) 982–994.
[13] S. Tyanova, T. Temu, J. Cox, The MaxQuant computational platform for mass spectrometry-based shotgun proteomics, Nat. Protoc. 11 (2016) 2301–2319.
[14] J. Cox, N. Neuhauser, A. Michalski, R.A. Scheltema, J.V. Olsen, M. Mann, Andromeda: a peptide search engine integrated into the MaxQuant environment, J. Proteome Res. 10 (2011) 1794–1805.
[15] B. Schwanhausser, D. Busse, N. Li, G. Dittmar, J. Schuchhardt, J. Wolf, et al., Global quantification of mammalian gene expression control, Nature 473 (2011) 337–342.
[16] J. Chen, E.E. Bardes, B.J. Aronow, A.G. Jegga, ToppGene Suite for gene list enrichment analysis and candidate gene prioritization, Nucleic Acids Res. 37 (2009) W305–W311.
[17] A. Subramanian, P. Tamayo, V.K. Mootha, S. Mukherjee, B.L. Ebert, M.A. Gillette, et al., Gene set enrichment analysis: a knowledge-based approach for interpreting genome-wide expression profiles, Proc. Natl. Acad. Sci. U. S. A. 102 (2005) 15545–15550.
[18] M. Uhlen, E. Bjorling, C. Agaton, C.A. Szigyarto, B. Amini, E. Andersen, et al., A human protein atlas for normal and cancer tissues based on antibody proteomics, Mol. Cell. Proteomics 4 (2005) 1920–1932.
[19] P. Bankhead, M.B. Loughrey, J.A. Fernandez, Y. Dombrowski, D.G. McArt, P.D. Dunne, et al., QuPath: open source software for digital pathology image analysis, Sci. Rep. 7 (2017) 16878.
[20] C. Manini, J.C. Angulo, J.I. Lopez, Mimickers of urothelial carcinoma and the approach to differential diagnosis, Clin. Pract. 11 (2021) 110–123.
[21] G. Sjodahl, M. Lauss, K. Lovgren, G. Chebil, S. Gudjonsson, S. Veerla, et al., A molecular taxonomy for urothelial carcinoma, Clin. Cancer Res. 18 (2012) 3377–3386.
[22] N. Xu, Z. Yao, G. Shang, D. Ye, H. Wang, H. Zhang, et al., Integrated proteogenomic characterization of urothelial carcinoma of the bladder, J. Hematol. Oncol. 15 (2022) 76.
[23] A.G. Robertson, J. Kim, H. Al-Ahmadie, J. Bellmunt, G. Guo, A.D. Cherniack, et al., Comprehensive molecular characterization of muscle-invasive bladder cancer, Cell 171 (2017) 540–556 e525.

[24] G.J. Netto, M.B. Amin, D.M. Berney, E.M. Comperat, A.J. Gill, A. Hartmann, et al., The 2022 World Health organization classification of tumors of the urinary system and male genital organs-Part B: prostate and urinary tract tumors, Eur. Urol. 82 (2022) 469–482.
[25] K.S. Li, X.D. Zhu, H.D. Liu, S.Z. Zhang, X.L. Li, N. Xiao, et al., NT5DC2 promotes tumor cell proliferation by stabilizing EGFR in hepatocellular carcinoma, Cell Death Dis. 11 (2020) 335.
[26] X. Jin, X. Liu, Z. Zhang, L. Xu, NT5DC2 suppression restrains progression towards metastasis of non-small-cell lung cancer through regulation p53 signaling, Biochem. Biophys. Res. Commun. 533 (2020) 354–361.
[27] Z. Zhu, Q. Hou, H. Guo, NT5DC2 knockdown inhibits colorectal carcinoma progression by repressing metastasis, angiogenesis and tumor-associated macrophage recruitment: a mechanism involving VEGF signaling, Exp. Cell Res. 397 (2020) 112311.
[28] A.J. Ridley, Rho GTPases and actin dynamics in membrane protrusions and vesicle trafficking, Trends Cell Biol. 16 (2006) 522–529.
[29] A.P. Wheeler, A.J. Ridley, Why three Rho proteins? RhoA, RhoB, RhoC, and cell motility, Exp. Cell Res. 301 (2004) 43–49.
[30] L. Jin, W.R. Liu, M.X. Tian, X.F. Jiang, H. Wang, P.Y. Zhou, et al., CCL24 contributes to HCC malignancy via RhoB- VEGFA-VEGFR2 angiogenesis pathway and indicates poor prognosis, Oncotarget 8 (2017) 5135–5148.
[31] M. Yoneda, Y.S. Hirokawa, A. Ohashi, K. Uchida, D. Kami, M. Watanabe, et al., RhoB enhances migration and MMP1 expression of prostate cancer DU145, Exp. Mol. Pathol. 88 (2010) 90–95.
[32] O. Calvayrac, A. Pradines, I. Raymond-Letron, I. Rouquette, E. Bousquet, V. Lauwers-Cances, et al., RhoB determines tumor aggressiveness in a murine EGFRL858R-induced adenocarcinoma model and is a potential prognostic biomarker for Lepidic lung cancer, Clin. Cancer Res. 20 (2014) 6541–6550.
[33] N. Wiedemann, N. Pfanner, Mitochondrial machineries for protein import and assembly, Annu. Rev. Biochem. 86 (2017) 685–714.
[34] F. Palmieri, The mitochondrial transporter family SLC25: identification, properties and physiopathology, Mol. Aspect. Med. 34 (2013) 465–484.
[35] F. Vetrini, S. McKee, J.A. Rosenfeld, M. Suri, A.M. Lewis, K.M. Nugent, et al., De novo and inherited TCF20 pathogenic variants are associated with intellectual disability, dysmorphic features, hypotonia, and neurological impairments with similarities to Smith-Magenis syndrome, Genome Med. 11 (2019) 12.